Journal of Instrumentation

PAPER • **OPEN ACCESS**

Characterization of plasmas in negative ion sources using a Cs-H Collisional Radiative model

To cite this article: B. Pouradier Duteil *et al* 2024 *JINST* **19** C02051

Published by IOP Publishing for Sissa Medialab

Received: *December 21, 2022*
Accepted: *January 14, 2024*
Published: *February 26, 2024*

8th International Symposium on Negative Ions, Beams and Sources
Orto Botanico, Padova, Italy
2–7 October 2022

Characterization of plasmas in negative ion sources using a Cs-H Collisional Radiative model

B. Pouradier Duteil,[a,b,*] M. Barbisan,[b] R. Milazzo,[b] C. Poggi,[b] E. Sartori,[b] M. Spolaore,[b] M. Ugoletti[c,b] and B. Zaniol[b]

[a] *Ecole Polytechnique Fédérale de Lausanne (EPFL), Swiss Plasma Center (SPC), CH 1015 Lausanne, Switzerland*
[b] *Consorzio RFX (CNR, ENEA, INFN, Università di Padova, Acciaierie Venete SpA), C.so Stati Uniti 4, 35127 Padova, Italy*
[c] *INFN-LNL, Viale dell'Università 2, 35020 Legnaro, Italy*

E-mail: basile.pouradierduteil@epfl.ch

Abstract: SPIDER, hosted at the Neutral Beam Test Facility (NBTF) in Padova, Italy, is the full scale prototype for the ITER Heating Neutral Beam (HNB) source. Another smaller compact RF ion source, NIO1, hosted by Consorzio RFX, was built to study the production and acceleration of H^- ions in continuous operation. Both machines operate with the evaporation of caesium in order to enhance the production of negative ions.

A collisional radiative model for caesium-hydrogen plasmas was recently developed. When used in conjunction with measurements from Optical Emission Spectroscopy, Laser Absorption Spectroscopy and electrostatic probes, the model can provide estimates of the plasma parameters with a good spatial resolution thanks to the many lines of sight available.

This work presents a characterization of the plasma in SPIDER and NIO1 using this method. In particular, we investigate the influence of the RF power and the magnetic filter field on the plasma properties, and compare the results with those of other source and beam diagnostics.

Keywords: Ion sources (positive ions, negative ions, electron cyclotron resonance (ECR), electron beam (EBIS)); Plasma diagnostics - interferometry, spectroscopy and imaging; Plasma diagnostics - probes

*Corresponding author.

https://doi.org/10.1088/1748-0221/19/02/C02051

2024 JINST 19 C02051

Contents

1 Introduction

The ITER experimental thermonuclear reactor will require at least two neutral beam injectors (NBI) for heating and current drive. These injectors are required to extract and accelerate beams up to 1 MeV for pulses lasting up to 3600 s [1], with currents densities of 330 A m^{-2} in the case of hydrogen and 285 A m^{-2} in the case of deuterium. SPIDER (Source for the Production of Ions of deuterium from a Radio frequency plasma) is the full-size prototype of the ITER NBI negative ion sources. It is hosted at the Neutral Beam Test Facility (NBTF) in Padova, Italy, and serves as an intermediate step before MITICA, the full-size prototype of ITER injectors [2]. Consorzio RFX also hosts the NIO1 experiment (Negative Ion Optimization 1), used as a training and research facility for studying negative ion source physics and diagnostics [3].

The ITER requirements for the NBIs cannot be met by volume-production of negative ions, SPIDER must therefore make use of an optimized surface-production, ie. charge exchange of positive ions or atoms with a converter surface. The negative ion production yield is greatly enhanced by reducing the surface's work function by evaporating caesium into the source [4].

The emission lines produced by the excited Cs atoms in the plasma can be measured through Optical Emission Spectroscopy (OES) [5, 6]. The intensity of these lines is a function of the volume density of Cs along the line of sight and of plasma parameters (n_e, T_e and n_{H^-}). A Collisional Radiative (CR) model was previously developed to help interpret the Cs emission lines in order to extract information on the Cs distribution in the source and on the plasma parameters [7].

NIO1 and SPIDER are both equipped with Laser Absorption Spectroscopy (LAS), a diagnostic dedicated to the measurement of the Cs ground state density [8]. Knowing the Cs ground state density, the CR model and OES measurements can be used to provide estimates of the plasma parameters. This work presents the use of this method to estimate the electron density in SPIDER and NIO1.

2024 JINST 19 C02051

2 Experimental setup and method

2.1 SPIDER

In SPIDER, the plasma is generated by 8 cylindrical drivers powered in pairs by 4 RF oscillators which can deliver up to 200 kW of power with an operating frequency of approximately 1 MHz. In the source, the plasma produced in the drivers propagates in the expansion chamber at the end of which lies the Plasma Grid (PG), serving as the first grid of the extraction and acceleration system as well as the main conversion surface for surface-production of negative ions. The survival probability of negative ions is enhanced by reducing the electron temperature in the extraction region by using a magnetic filter field produced by a current flowing through the PG in the vertical direction. The electric field in the region near the PG is optimized by varying the potential of a Bias Plate (BP) mounted 10 mm upstream of the PG. SPIDER is equipped with a large number of LoSs for OES, parallel to the PG or looking axially through the drivers. Figure 1 features the horizontal LoSs parallel to the PG at 5, 17, 35 and 65 mm from the PG as well as the four LoSs used for LAS at 25 mm from the PG. A measurement of the negative ion density is also provided by Cavity Ring Down Spectroscopy (CRDS) [9] at 5 mm from the PG. The data used in this contribution was collected during the first campaign with Cs evaporation. Near the grids, the electron temperature and density are rather low, and the Cs density is of the order of 10^{13}–10^{14} m^{-3} [10]. As as consequence, the Cs excited states are poorly populated, making most of the Cs emission lines difficult to distinguish from the rest of the spectrum and therefore difficult to accurately measure. The results shown in section 3 only utilize the most intense Cs emission line at 852 nm, corresponding to the $6^2P_{3/2} \rightarrow 6^2S_{1/2}$ de-excitation.

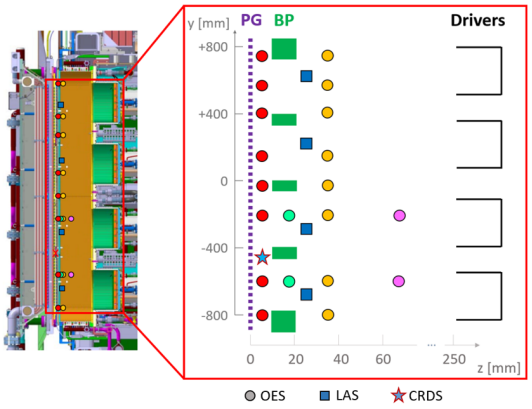

Figure 1. LoSs used for OES (circles), LAS (blue squares) and CRDS (star) in SPIDER.

In order to estimate n_e using the OES measurements and the CR model, assumptions on other plasma parameters are required. The electron temperature is set at 1.5 eV for the LoSs at 5 mm from the PG and at 2 eV for the LoSs at 35 mm from the PG. These numbers come from previous campaigns characterizing the plasma in SPIDER using movable electrostatic probes [11], and from measurements of electrostatic probes embedded in the PG and the BP [12].

In addition to the excitation caused by collisions with electrons, the Cs excited states are populated by the mutual neutralization of Cs^+ and H^-, especially when n_{H^-} reaches values similar or greater than n_e [13]. The importance of this channel is well documented, but including it requires assumptions on both n_{H^-} and n_{Cs^+}. SPIDER is equipped with a CRDS measurement of n_{H^-} near the PG, but this value is expected to vary substantially in the vertical direction as indicated by the vertical non-uniformity of the extracted H^- beam measured by the beam diagnostics. In section 3.2, the vertical profile of n_{H^-} will therefore be approximated as equal to the beam current vertical profile measured by the STRIKE diagnostic, normalized with the CRDS n_{H^-} measurements. No direct measurement of n_{Cs^+} is made in SPIDER, this quantity will be discussed further in section 3.

2.2 NIO1

The NIO1 experiment is a small, compact negative ion source used to study steady-state operation and serves as a research and training facility for diagnostics. The source is a 20 cm long cylinder with a diameter of 10 cm, powered by a single RF-driver providing up to 2.5 kW and operating at 2 MHz (figure 2). Similarly to SPIDER, the extraction system is made up of three grids, and Cs is injected in the source with a Cs oven. The plasma in the source is monitored via OES, with an axial line of sight, and the Cs ground state density is measured with LAS through a LoS looking parallel to the PG at a distance of 19 mm. During the last campaign in NIO1, the LoS parallel to the PG was often used by OES instead of LAS to study the Cs emissions in a colder plasma where the order of magnitude of the Cs ground state density was known.

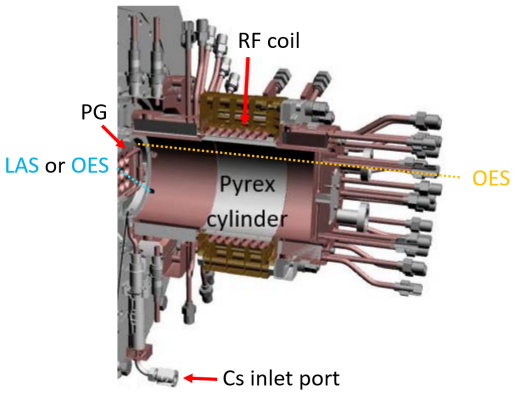

Figure 2. NIO1 setup and LoSs used for OES and LAS diagnostics.

3 Results in SPIDER

3.1 Comparison with Langmuir probe measurements and estimation of n_{Cs^+}

SPIDER is equipped with a set of Langmuir probes embedded in its PG and BP. Most of the probes are negatively polarized during the pulses with respect to their grid reference (i.e., PG or BP) to measure the positive-ion saturation current. A subset of the probes can also be polarized with voltage sweeping ramps to collect the current-voltage characteristic [14]. Figure 3(b) features the measurements of n_{H^-} by CRDS during an experimental day. The caesium density measured by LAS and the intensity of the 852 nm emission line at the closest LoSs are shown on figure 3(a). Using these measurements together with the CR model (with $T_e = 1.5$ eV), estimations of n_e are obtained for several hypotheses on the Cs ion-to-atom ratio. These values are compared with measurement of n_e made with one of the probes undergoing voltage sweeps located at the center of the bottom-most segment of the PG [15, 16], near the LoS dedicated to CRDS (figure 3(c)). The typical measurement uncertainties are of ±20% for OES and ±10% for CRDS and LAS.

At 5 mm from the PG, and especially in the bottom part of the source, the electronegativity of the plasma is usually very large. This is also the case in this particular set of data, where n_{H-}/n_e can reach values of the order of 10 [15]. In these conditions, the results of the CR model are extremely sensitive to the hypothesis made on the Cs^+ density, as seen in figure 3(c). The absence of certain points in the case $n_{Cs^+}/n_{Cs^0} = 2$ (e.g. at ~17:02 or after 18:00) is due to the fact that, in the model, mutual neutralization alone is sufficient to populate the $6^2P_{3/2}$ level at densities corresponding to those measured with the 852 nm line, resulting in an unrealistic $n_e = 0\,\mathrm{m}^{-3}$.

The general trend of n_e estimated by the Cs OES-CR model method is similar to what is measured with the Langmuir probes, with an overall decrease throughout the operational day, and low electron densities after long pauses without plasma (e.g. at ~ 16:00, 17:00 and 18:15). The absolute values of n_e approach the values measured with the Langmuir probe when $\frac{n_{Cs^+}}{n_{Cs^0}}$ is set between 1.5 and 2. However this comparison demonstrates that, at least at the PG where electronegativity is large,

2024 JINST 19 C02051

a precise assessment of the Cs^+ density is required in order to give a reasonable estimation of n_e with the Cs OES-CR model method.

Such a comparison could not be made at the BP: unlike the probes in the PG, those embedded in the BP did not undergo voltage sweeps and only measured the ion saturation current during the pulses discussed in this work. We expect the Cs ion-to-atom ratio to be larger at the BP, but the importance of the mutual neutralization of Cs^+ and H^- in populating the Cs excited states should decrease with respect to electron excitation, as n_e rises and n_{H^-} decreases when moving away from the grids.

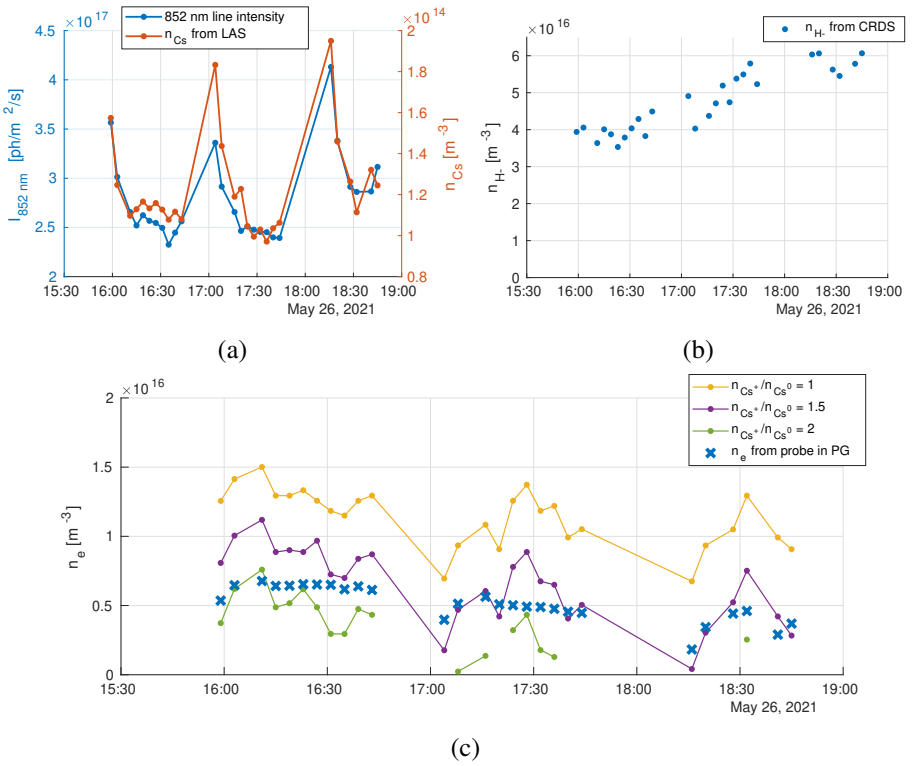

Figure 3. (a) OES measurement of the 852 nm Cs emission line (at 5 mm from PG) and LAS measurement of n_{Cs}, (b) n_{H^-} measured by CRDS, (c) n_e measured by the method combining OES & CR model for 3 different Cs ion-to-atom ratios, compared with measurements of n_e made with a Langmuir probe embedded in the PG (SPIDER parameters: $P_{RF} = 4 \times 100$ kW, $I_{PG} = 1.5$ kA, $I_{ISBI} = I_{ISBP} = 80$ A, $\Gamma_{Cs} = 12$ mg/h).

3.2 Characterization of the electron density during machine parameter scans

The many LoSs available on SPIDER can be used to perform profiles of the electron density with the OES-CR model method. Figure 4 shows the effect that the inversion of the direction of the magnetic filter field has on n_e. Figure 4(a) features the OES measurement of the Cs 852 nm emission line at several vertical positions (at 35 mm from the PG), as well as the Cs and H^- densities extrapolated from the LAS and CRDS measurements used as input to the model. Figure 4(b) presents the resulting estimations of n_e, using two hypotheses on the density of Cs^+. The electron density in the standard configuration presents a large non-uniformity, with n_e at the bottom of the source reaching ~ 4 times the value at the top. The low values of n_e at $y \approx 0$ mm and $y \approx 400$ mm are due to the fact that these LoSs are located between pairs of drivers and therefore see a weaker plasma. Inverting the filter-field causes a moderate increase of n_e at the bottom of the source, and a very large increase of n_e at the top.

2024 JINST 19 C02051

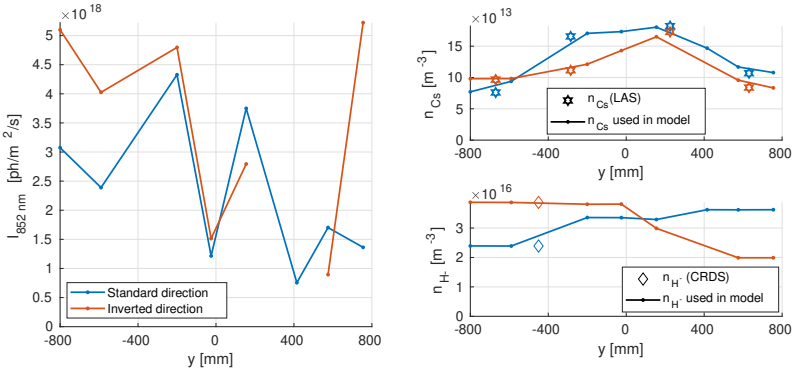

(a)

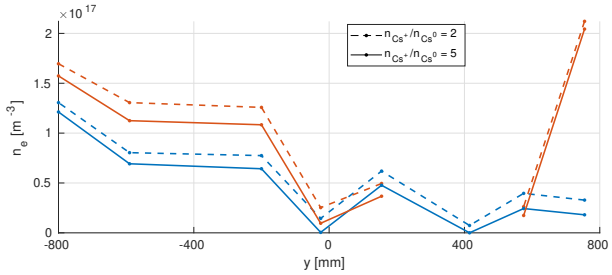

(b)

Figure 4. Inversion of the magnetic filter field direction — (a) Measurements and hypotheses, (b) n_e estimated with the OES-CR model method using $n_{Cs^+}/n_{Cs^0} = 2$ or 5 ($I_{PG} = 1.05\,kA$, $I_{ISBI} = 190\,A$, $I_{ISBP} = 0\,A$, $\Gamma_{Cs} = 12\,mg/h$).

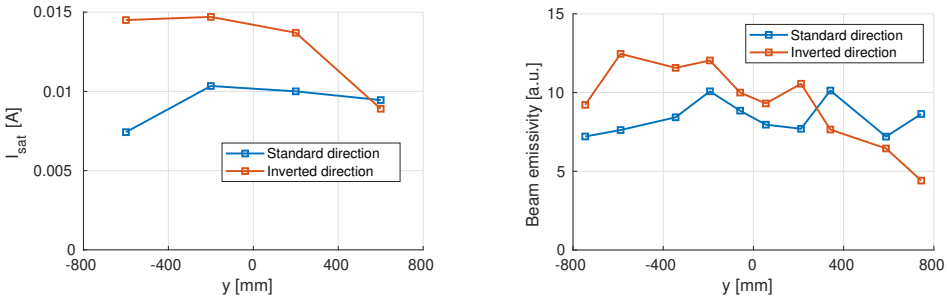

(a) (b)

Figure 5. Effect of the inversion of the filter field on (a) ion saturation current ($\propto n_+$) measured by probes embedded in the BP and (b) emissivity of the beam measured by visible cameras.

The ion saturation current, proportional to n_+, measured by electrostatic probes embedded in the BP is shown on figure 5(a). The inversion of the filter field seems to increase the positive ion density everywhere but in the upper part of the source where n_+ remains unchanged. Assuming that $n_+ \sim n_e + n_{H^-}$, this implies that the strong increase of n_e in the upper part of the source shown in figure 4(b) must be accompanied by a decrease of n_{H-}, which is consistent with measurements of the emissivity of the beam with visible cameras [17] indicating a decrease of the extracted current in the upper beamlets after inversion of the filter field (figure 5(b)).

2024 JINST 19 C02051

Figure 6 shows estimations of n_e using the OES-CR model method for three RF powers, keeping the other machine parameters constant. The effect of the increase of the RF power on the electron density is clearly seen, with n_e increasing by a factor of 2–3 when going from 4×45 kW to 4×100 kW.

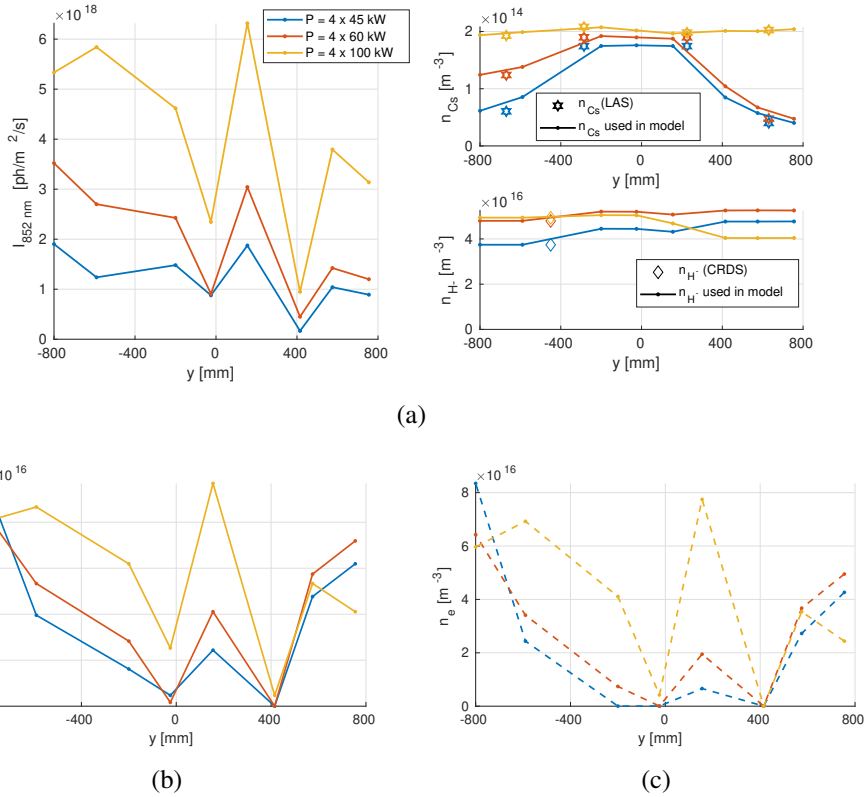

Figure 6. RF power scan — (a) Measurements and hypotheses, (b) n_e estimated with the OES-CR model method using $n_{Cs^+}/n_{Cs^0} = 2$, (c) n_e estimated with the OES-CR model method using $n_{Cs^+}/n_{Cs^0} = 5$ ($I_{PG} = 1.2$ kA, $I_{ISBI} = I_{ISBP} = 80$ A, $\Gamma_{Cs} = 12$ mg/h).

4 Results in NIO1

The OES spectra measured on NIO1 feature many more Cs emission lines than in SPIDER. This is likely due to a combination of a greater temperature near the grids and a Cs ground state density orders of magnitude greater than what is measured in SPIDER [18] (the LAS diagnostic measures $n_{Cs} \sim 10^{16}\,m^{-3}$ in NIO1 and $\sim 10^{14}\,m^{-3}$ in SPIDER).

Figure 7 features an example of the Cs emission lines (absolutely calibrated) measured in NIO1, with the OES LoS in front of the PG (the y-axis is in logarithmic scale in order to better visualize all of the lines). The uncertainty is estimated at $\sim 5-10\%$ of the measured value. The intensity of the Cs lines varies with the total Cs density and the plasma parameters: qualitative information on the plasma parameters can be obtained by looking at the ratios of the emission lines, which eliminates the dependency of their intensities on the Cs ground state density.

2024 JINST 19 C02051

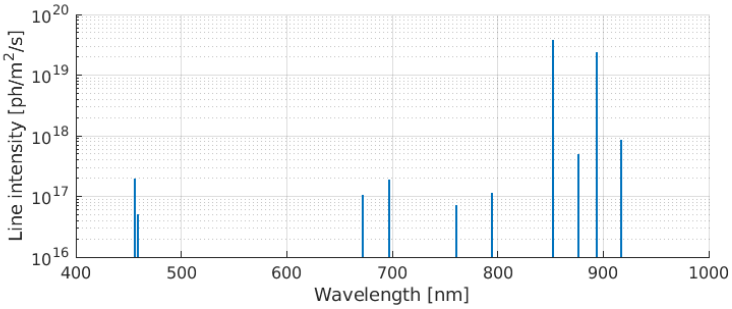

Figure 7. Example of Cs lines measured in NIO1 (p = 3 Pa, P = 1400 W, I_{PG} = 10 A, V_{bias} = 25 V).

Not all Cs line ratios are sensitive to changes in electron temperature or density. Looking at the de-excitation channels that correspond to the emission lines measured by spectroscopy (figure 8) one can intuitively understand that, although they are the most intense and well-defined peaks in the emission spectra, looking at the ratio between the 852 nm and 894 nm peaks will provide little information as they originate from very similar de-excitations ($6^2P_{3/2} \rightarrow 6^2S_{1/2}$ and $6^2P_{1/2} \rightarrow 6^2S_{1/2}$), and the same goes for the $\frac{697\,\text{nm}}{672\,\text{nm}}$ ratio. On the other hand, we expect the $\frac{672\,\text{nm}}{894\,\text{nm}}$, $\frac{697\,\text{nm}}{894\,\text{nm}}$, $\frac{876\,\text{nm}}{894\,\text{nm}}$ or $\frac{876\,\text{nm}}{459\,\text{nm}}$ ratios to change with varying plasma temperature and densities. Figures 9(a) and 9(b) show the dependency of these Cs line ratios on plasma parameters in the simulations made with the CR model. The $\frac{672\,\text{nm}}{894\,\text{nm}}$, $\frac{697\,\text{nm}}{894\,\text{nm}}$ and $\frac{876\,\text{nm}}{894\,\text{nm}}$ ratios all seem to increase with the electron density and temperature. As expected, the $\frac{852\,\text{nm}}{894\,\text{nm}}$ and $\frac{697\,\text{nm}}{672\,\text{nm}}$ ratios have little to no dependency on T_e and n_e, while the $\frac{876\,\text{nm}}{459\,\text{nm}}$ ratio seems to increase with increasing n_e and decrease with increasing T_e, making it difficult to interpret.

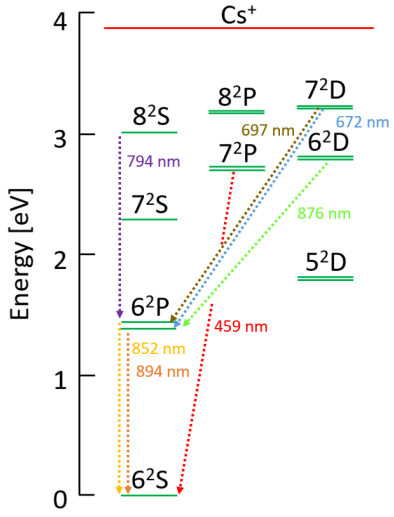

Figure 8. Emission channels corresponding to main Cs peaks seen in NIO1.

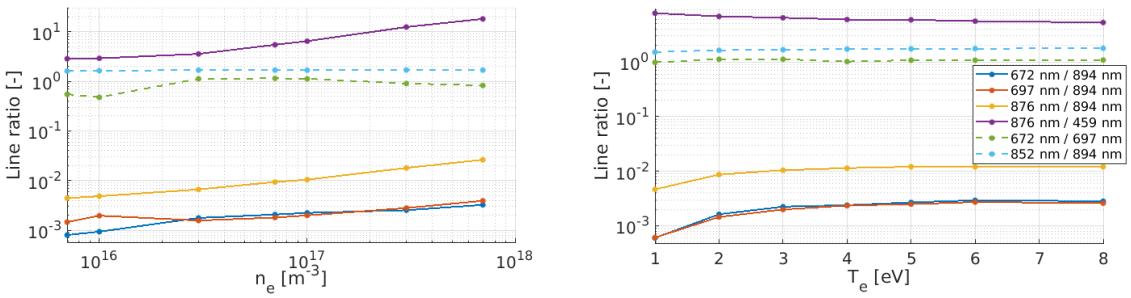

(a) (b)

Figure 9. Dependency of simulated Cs emission line ratios on (a) n_e (with T_e = 3 eV, $n_{H^-} = 2 \cdot 10^{15}\,\text{m}^{-3}$, $n_{Cs^+}/n_{Cs^0} = 5$) and (b) T_e (with $n_e = 10^{17}\,\text{m}^{-3}$, $n_{H^-} = 2 \cdot 10^{15}\,\text{m}^{-3}$, $n_{Cs^+}/n_{Cs^0} = 5$).

These emission line ratios can therefore be used to make qualitative assessments about the plasma. Figure 10(a) shows several line ratios taken from three spectra measured during a pressure scan in NIO1. The evolution of the ratios with increasing pressure can be better visualized by plotting their relative change with respect to their value at p = 1.5 Pa (figure 10(b)). The ratios undergo an overall decrease with increasing pressure, which points towards a decrease of the electron density and/or temperature. However, the changes in the ratios' values is rather limited, decreasing of 20% at most with respect to their value at 1.5 Pa, which implies that the electron density and temperature underwent only minor changes during this pressure scan.

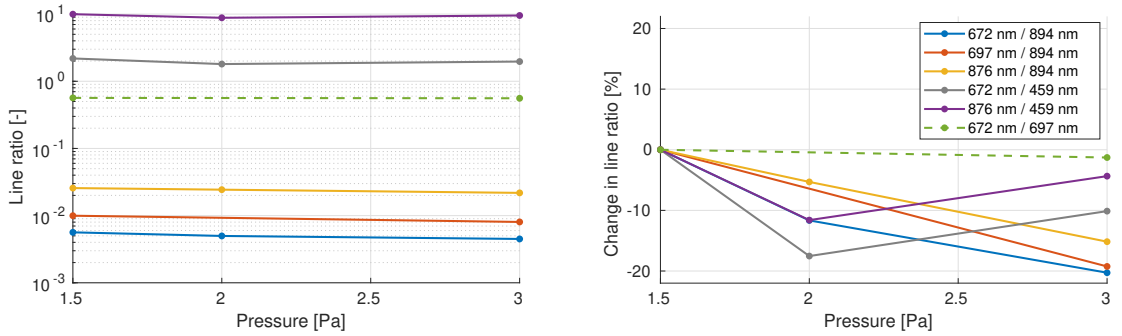

(a) (b)

Figure 10. Cs line ratios measured in NIO1 during a pressure scan (P = 1600 W, V_{bias} = 25 V, I_{PG} = 10 A).

As in SPIDER, estimates of the electron density can be made using hypotheses on the electron temperature, negative ion density and Cs ground-state density. Electric probe measurements made during a previous experimental campaign provided typical values of $T_e \sim 4$–5 eV and $n_e \sim 10^{17}$ m^{-3} (without Cs) at 2 cm from the PG where the spectroscopy LoS is located [19]. However the magnetic filter field in NIO1 was recently modified in order to further reduce the electron temperature near the PG, we therefore set $T_e \sim 3$ eV.

NIO1 is not yet equipped with any diagnostic capable of measuring the H^- density. Serianni et al. [20] showed that, in SPIDER, a good agreement could be obtained between measurements of n_{H^-} and estimates from the beam current using the following approximation:

$$j_b = \frac{A}{A_0} h \sqrt{\frac{k_B T_+}{m_-}} e n_{H^-,b} \tag{4.1}$$

where j_b [A/m^2] is the beam current density, A [m^2] the meniscus area, A_0 [m^2] the aperture area, $h = \exp(-e\Delta V / k_B T_+)$ with ΔV [V] the pre-sheath voltage, T_+ [K] the temperature of positive ions, m_- [kg] the mass of negative ions and $n_{H^-,b}$ [m^{-3}] the negative ion density in front of the aperture. Finally, LAS measurements before and after the scan saw a Cs ground-state density of the order of $\sim 1.5 \cdot 10^{16}$ m^{-3}.

Combining these hypotheses with the OES measurements and the CR model, estimates of the electron density can be obtained and are shown in table 1. These numbers must be considered cautiously as strong hypotheses on several other parameters were required, but the order of magnitude is consistent with the previous Langmuir probe campaigns in NIO1. As implied by the Cs line ratios shown in figure 10, increasing the pressure seems to cause a decrease of n_e, with an estimated $\sim$ 30% decrease when going from 1.5 Pa to 3 Pa.

2024 JINST 19 C02051

Table 1. Estimation of n_e during a pressure scan (P = 1600 W, V_{bias} = 25 V, I_{PG} = 10 A).

Pressure [Pa]	T_e [eV]	n_{H-} [m^{-3}]	n_{Cs^+}/n_{Cs^0} [-]	n_{Cs^0} [m^{-3}]	$\mathbf{n_e}$ [$\mathbf{m^{-3}}$]
1.5	3	$2 \cdot 10^{15}$	5	$1.5 \cdot 10^{16}$	$\mathbf{1.6 \cdot 10^{17}}$
2	3	$3.5 \cdot 10^{15}$	5	$1.5 \cdot 10^{16}$	$\mathbf{1.25 \cdot 10^{17}}$
3	3	$5 \cdot 10^{15}$	5	$1.5 \cdot 10^{16}$	$\mathbf{1.1 \cdot 10^{17}}$

5 Conclusion

A Collisional Radiative model for hydrogen-caesium plasmas was used in conjunction with measurements of Optical Emission Spectroscopy to estimate the electron density in negative ion sources. In SPIDER, comparisons with measurements of electrostatic probes were made and provided an estimate of the Cs ion-to-atom ratio of 1.5–2 at 5 mm from the Plasma Grid. The behavior of n_e when increasing the RF power and inverting the magnetic filter field direction was studied and found to be consistent with measurements by other diagnostics. In NIO1, the detection of many Cs emission lines allowed for qualitative assessments of the behavior of the plasma when changing the pressure or RF power, and estimates of the electron density were found to be of the same order of magnitude of electrostatic probe measurements made during previous campaigns and consistent with the expected behavior of the plasma.

Acknowledgments

This work has been carried out within the framework of the ITER-RFX Neutral Beam Testing Facility (NBTF) Agreement and has received funding from the ITER Organization. The views and opinions expressed herein do not necessarily reflect those of the ITER Organization.

This work has been carried out within the framework of the EUROfusion Consortium, funded by the European Union via the Euratom Research and Training Programme (Grant Agreement No 101052200 — EUROfusion). Views and opinions expressed are however those of the author(s) only and do not necessarily reflect those of the European Union or the European Commission. Neither the European Union nor the European Commission can be held responsible for them.

This work was supported in part by the Swiss National Science Foundation.

References

[1] V. Toigo et al., *The PRIMA test facility: SPIDER and MITICA test-beds for ITER neutral beam injectors*, *New J. Phys.* **19** (2017) 085004.

[2] V. Toigo et al., *On the road to ITER NBIs: SPIDER improvement after first operation and MITICA construction progress*, *Fusion Eng. Des.* **168** (2021) 112622.

[3] M. Cavenago et al., *The NIO1 negative ion source: Investigation and operation experience*, *AIP Conf. Proc.* **2052** (2018) 040013.

[4] Y. Belchenko, G. Dimov and V. Dudnikov, *A powerful injector of neutrals with a surface-plasma source of negative ions*, *Nucl. Fusion* **14** (1974) 113.

[5] B. Zaniol, M. Barbisan, D. Bruno, R. Pasqualotto, C. Taliercio and M. Ugoletti, *First measurements of optical emission spectroscopy on SPIDER negative ion source*, *Rev. Sci. Instrum.* **91** (2020) 013103.

[6] U. Fantz et al., *Diagnostics of the cesium amount in an RF negative ion source and the correlation with the extracted current density*, *Fusion Eng. Des.* **74** (2005) 299.

[7] B. Pouradier Duteil et al., *Development of a collisional radiative model for hydrogen-cesium plasmas and its application to SPIDER*, *IEEE Trans. Plasma Sci.* **50** (2022) 3995.

[8] M. Barbisan, S. Cristofaro, L. Zampieri, R. Pasqualotto and A. Rizzolo, *Laser absorption spectroscopy studies to characterize cs oven performances for the negative ion source SPIDER*, 2019 *JINST* **14** C12011.

[9] M. Barbisan et al., *Negative ion density in the ion source SPIDER in cs free conditions*, *Plasma Phys. Control. Fusion* **64** (2022) 065004.

[10] E. Sartori et al., *First operations with caesium of the negative ion source SPIDER*, *Nucl. Fusion* **62** (2022) 086022.

[11] E. Sartori et al., *Development of a set of movable electrostatic probes to characterize the plasma in the ITER neutral beam negative-ion source prototype*, *Fusion Eng. Des.* **169** (2021) 112424.

[12] M. Spolaore, G. Serianni, A. Leorato and F.D. Agostini, *Design of a system of electrostatic probes for the RF negative ion source of the SPIDER experiment*, *J. Phys. D* **43** (2010) 124018.

[13] D. Wünderlich, C. Wimmer and R. Friedl, *A collisional radiative model for low-pressure hydrogen-caesium plasmas and its application to an RF source for negative hydrogen ions*, *J. Quant. Spectrosc. Radiat. Transf.* **149** (2014) 360.

[14] C. Poggi et al., *Langmuir probes as a tool to investigate plasma uniformity in a large negative ion source*, *IEEE Trans. Plasma Sci.* **50** (2022) 3890.

[15] C. Poggi et al., *Highly electronegative plasma conditions in the SPIDER negative ion source*, submitted to *Fusion Eng. Des.*.

[16] J. Bredin, P. Chabert and A. Aanesland, *Langmuir probe analysis in electronegative plasmas*, *Phys. Plasmas* **21** (2014) 123502.

[17] M. Ugoletti, M. Agostini, A. Pimazzoni, E. Sartori and G. Serianni, *Spider beam homogeneity characterization through visible cameras*, *IEEE Trans. Plasma Sci.* **50** (2022) 3913.

[18] M. Barbisan et al., *Cs evaporation in a negative ion source and Cs cleaning tests by plasma sputtering*, *IEEE Trans. Plasma Sci.* **50** (2022) 3859 [arXiv:2308.15328].

[19] P. Veltri et al., *Langmuir probe characterization of the NIO1 ion source plasma*, *AIP Conf. Proc.* **2011** (2018) 050011.

[20] G. Serianni et al., *Spatially resolved diagnostics for optimization of large ion beam sources*, *Rev. Sci. Instrum.* **93** (2022) 081101.

2024 JINST 19 C02051